Compact very low temperature scanning tunneling microscope with mechanically driven horizontal linear positioning stage

H. Suderow,[a] I. Guillamon, and S. Vieira
Laboratorio de Bajas Temperaturas, Departamento de Física de la Materia Condensada Instituto de Ciencia de Materiales Nicolás Cabrera, Facultad de Ciencias Universidad Autónoma de Madrid, 28049 Madrid, Spain

(Received 3 December 2010; accepted 19 February 2011; published online 23 March 2011)

We describe a scanning tunneling microscope for operation in a dilution refrigerator with a sample stage which can be moved macroscopically in a range up to a cm and with an accuracy down to the tens of nm. The position of the tip over the sample as set at room temperature does not change more than a few micrometers when cooling down. This feature is particularly interesting for work on micrometer sized samples. Nanostructures can be also localized and studied, provided they are repeated over micrometer sized areas. The same stage can be used to approach a hard single crystalline sample to a knife and cleave it, or break it, *in situ*. *In situ* positioning is demonstrated with measurements at 0.1 K in nanofabricated samples. Atomic resolution down to 0.1 K and in magnetic fields of 8 T is demonstrated in $NbSe_2$. No heat dissipation nor an increase in mechanical noise has been observed at 0.1 K when operating the slider. © *2011 American Institute of Physics*. [doi:10.1063/1.3567008]

I. INTRODUCTION

At present only few scanning probe microscopes (SPM), which can be operated well below 1 K, have been reported.[1–9] Those adapted to dilution refrigerators seem to be most interesting, as this technology is unique in providing a cold point stable in time that can cool down large devices to temperatures which are 1 or 2 orders of magnitude below 1 K. Moreover, it can be easily combined with high magnetic field setups, and the recent advances in pulse tube technology have considerably simplified its operation.[10,11] Very low temperature SPM offers surface characterization possibilities in, e.g., quantum nanostructures in semiconductors or in superconductors. A SPM is usually based on a microscopic probe, e.g., a tip in a tunneling microscope, which is mounted on a piezotube,[12] or a compact set of piezostacks, and scanned with respect to a sample attached to a holder. The position of the probe on top of the sample holder is controlled via coarse approach (Fig. 1).

The cryogenic environment is inherently inadequate to the SPM. The needed flow of cryogenic liquid through large amount of piping, and several room temperature located pumps, produces mechanical vibrations which are difficult to filter out or avoid without decreasing to some extent the cooling capacities of the refrigerator. These mechanical vibrations can lead to changes in the position of the probe with respect to the sample, producing noise in the SPM. The probe–sample system is held together through the coarse approach. Therefore, to operate a SPM at low temperatures, the coarse approach mechanisms should be designed carefully. If they are rigid enough, the SPM will have a high resonance frequency and this will decouple the probe–sample system from the mostly low frequency vibrations of the cryogenic devices. In addition, the coarse motor should dissipate the smallest possible amount of heat to allow continuous operation at the lowest temperatures.

[a]Electronic mail: Hermann.suderow@uam.es.

Several cryogenic step-by-step or inertial stip-slick piezoelectric motors have been built.[14–24] The use of piezoelectrics for precisely scanning over the sample is unparalleled in terms of reliability and accuracy.[25–27] However, their use in motors for coarse positioning bears some problems. The motor consists generally of a moving holder which is attached using a spring or an elastic membrane to a base, through piezoelectric ceramics. The holder is attached as firmly as possible—using, e.g., a strong spring and taking advantage of the friction between the surface of the holder with the piezoelectric ceramic arrangement—to allow for the highest possible mechanical stability. However, it must be free enough for inertial or step-by-step motion. In inertial stip-slick motors, when the acceleration of the holder produced by the piezo is high, the inertial force will win over friction and the holder will stay on its position. When the piezo moves slowly, the friction force will move the holder.[28] Thus, typically friction shall not be too strong, and the piezos should move as much and as fast as possible. When cooling, changes in the strain coefficients of the piezoceramics lead to a significant decrease of the range of motion, often a factor of 5 or 6.[26,29] Therefore, the motor cannot be operated as effectively as in a room temperature design. Generally, the friction is reduced to allow for low temperature operation, so that the stability of the design is also reduced. Moreover, a relatively high frequency ac voltage drive is needed. This implies strong heat dissipation at the capacitors formed by the piezoceramics. Although losses in capacitors are usually low, the power generated by the ac signal is certainly in the tens of mW range in a typical motor. It is then unavoidable that the holder is heated during operation and it is necessary to wait tens of minutes until it cools down again. On the other hand, when such coarse positioning devices are used to change the scanning window (as, e.g., an x–y table), it can happen that they tend to drift away when cooling down, changing the position of the probe over the sample holder over some tens of micrometers. In such a case, to find again a micrometer sized sample *in situ*,

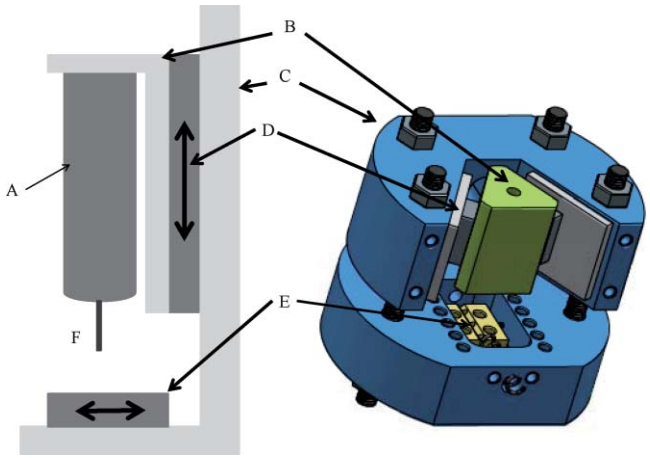

FIG. 1. (Color online) Schematics of a typical SPM setup for cryogenic environment (left panel) and a drawing of one possible design (right panel). A piezotube or a series of piezostacks (A in left panel) are used for fine scanning and positioning of a local probe sensing arrangement down to subatomic distances and at ranges up to some micron at low temperatures. In the right panel, the piezotube is not shown. It is mounted within its frame (the prism B), with the free end for scanning at the bottom. As a local probe we show in the left panel a tip for a tunneling microscope (STM, F in left panel, not shown in right panel), but this may carry another device, as, e.g., a tuning fork resonator for AFM (Ref. 13). The frame (B) is itself connected through a coarse Z approach (D) to another frame (C). Eventually, the sample holder is mounted on another coarse positioning system (E), which may allow for *X* or *X*–*Y* positioning of the tip.

at low temperatures, becomes a problem which needs careful consideration.

Here we propose to solve these problems through a new coarse approach device adapted to dilution refrigerator scanning tunneling microscopes (STM). The coarse approach allows for nanometer size motion over a range that can go up to cm, without heating effects and with an excellent mechanical stability. We show the proof of concept by using a STM setup with a piezo driven coarse Z approach and attach to it a sample holder with the new mechanical coarse positioner. We discuss different aspects of the device and successful experiments made in nanofabricated structures and at high magnetic fields.

II. DESCRIPTION OF THE CRYOGENIC SETUP

The cryogenic setup consists of a classical dilution refrigerator with 25 μW cooling power at 100 mK, inserted into the bore of a superconducting magnet (Fig. 2).[30] The superconducting magnet has a compensated field region located close to the mixing chamber to reduce Foucault current heating and provide for a field free region for thermometry. The dilution insert is surrounded by a sliding seal which allows for rapid heating of only the insert, giving, in practice, turn around times of around some hours for changing sample and going back to lowest temperatures. Pumps are located about 5 m away and are vibration isolated by use of silicone tubing, sand boxes, and rubber shells around stainless steel flexible pumping lines. A sound insulating foam is glued to the outside of the nitrogen-free dewar.

The vacuum chamber for the dilution refrigerator and STM consists of a conventional indium sealed circular closed tubing assembly, which is immersed into liquid helium. The helium level is usually located well below the upper flange of the vacuum chamber. The helium pick-up capillary is vacuum insulated to allow for helium flow into the 1 K pot, as usual in refrigerators of the type of Ref. 30. This has the advantage that, with the same length, more space is left free for the experiment. However, the temperature of the upper flange needs to be as close as possible to liquid helium temperatures, to avoid complex thermalization arrangements for wires inside the vacuum chamber at the 1 K pot. Usually, the vacuum chamber is built from stainless steel and a copper jacket is welded in a few points to the upper flange. This allows for operation of the fridge, but the amount of liquid helium needed to cool the vacuum chamber is high, due to the weight of the stainless steel vacuum chamber and the copper jacket. Here, we use instead a vacuum chamber totally made of a high thermal conductivity material with low weight, such as Al. This maintains the temperature of the upper flange below 10 K. The amount needed to cool liquid helium is reduced by about a factor of 3.[31] Moreover, the time needed to change the sample, heating and cooling again the insert, is reduced to half the time needed to do the same operation with a conventional vacuum chamber.

The wires for thermometry and STM are inserted into tubing connected to the low temperature vacuum chamber. On top, at room temperature, they are soldered to the electrical vacuum feed through connection. All lines have to be filtered at room temperature from radio frequency interference (RFI), to avoid overheating effects in thermometry and spectroscopy with all the filters as close as possible to the cryostat. However, it is convenient to be able to change the filtering circuitry to optimize the bandwidth of each connection. This implies that some mm in space are needed for each electrical connection, to be able to accommodate feed through capacitors, resistors, and inductors. To optimize the available space and bring the RFI filters as close as possible to the top of the

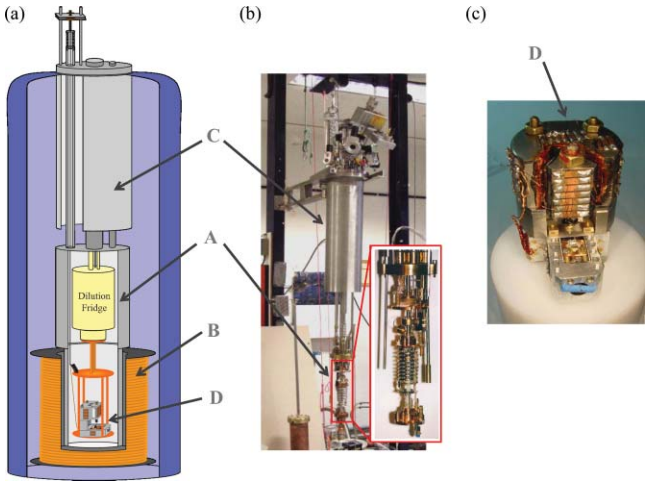

FIG. 2. (Color online) In (a), an overall schematics of the STM within the dilution refrigerator (A) and magnetic field coil (B) is shown. Corresponding photography is shown in (b). The dilution refrigerator has a sliding seal arrangement (C), which allows for a fast turn around time. In (c), we show a photograph of the low temperature STM head (D), which is thermally linked to the coldest point of the dilution fridge.

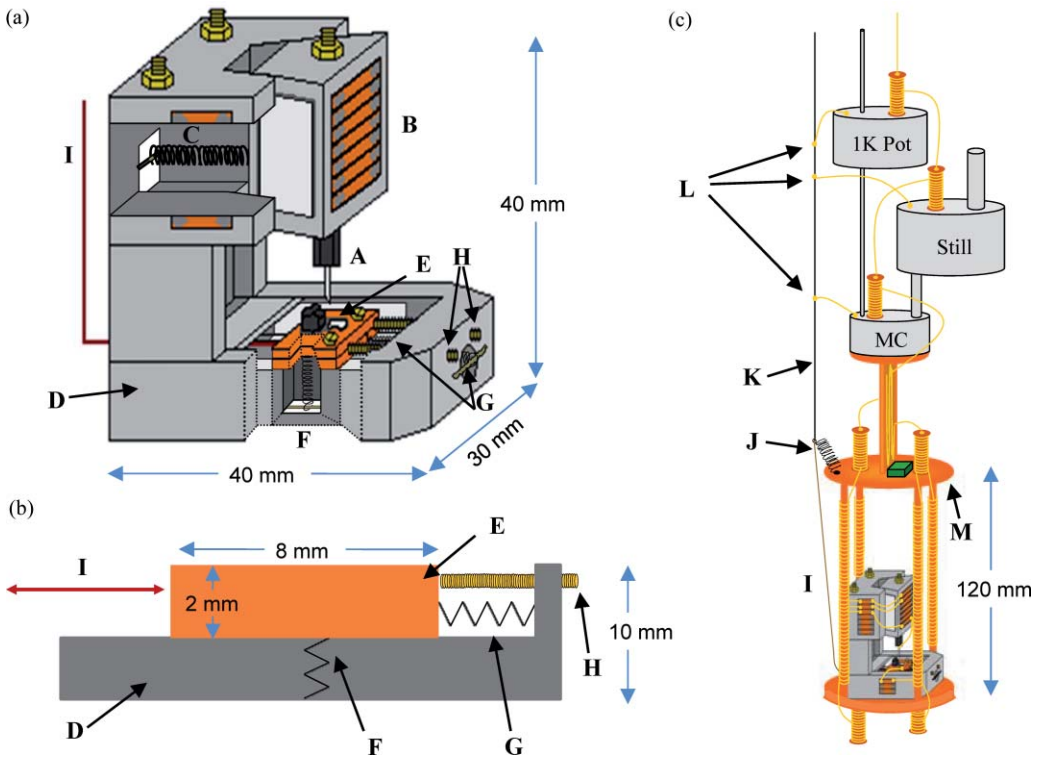

FIG. 3. (Color online) In (a), a representation of the overall setup used to prove the concept of the new motion unit. The tip (A) is hanging on the bottom of the piezotube, which is mounted on a prism (B, see also Fig. 1, right panel). The spring (C) fixes the prism to the main frame (D), and piezostacks are glued on the support, to make an inertial motor used to approach the tip to the sample. The positioning unit to move in the scanning plane is screwed at the bottom [a schematic lateral view is shown in (b)]. It consists of a slider (E), fixed using springs (F and G) to the support (D). The slider moves on a track, constructed as a wedge directed to the bottom (into D) to remove degrees of freedom perpendicular to the motion. Alumina covered with graphite are located within the track and at the slider, in the contact points between both. The sample holder is screwed to the slider. Additional screws (H) serve to position the slider in the scanning plane prior to cool down. The Kevlar rope (I) serves to pulls on the slider (D), and a stainless steel wire [K, in (c)] pulls on the Kevlar rope. The stainless steel wire is attached to a support [M, in (c)] below the mixing chamber of the dilution refrigerator with a spring [J, in (c)] and then thermalized at different positions (L). Mixing chamber, still and 1 K pot are schematically represented by the grey cylinders. Overall dimensions are given.

cryostat, we have used a home made vacuum feed through which can be mounted directly on a classical O-ring vacuum connection. The size of the feed through system has been adjusted to the available vacuum connections, and the RFI filter circuitry has been easier to locate close to the entrance to the vacuum chamber than when using commercially available hermetic connectors.

Temperature control is made using Air Liquide TRMC2 controller.[32] Below the mixing chamber, stable and homogeneous temperature is guaranteed by the use of copper supports, with a heater on top of them. We use Matshushita, calibrated Ge, and carbon CCS sensors[33–35] and locate some of them close to the mixing chamber, at the zero field region of the compensated superconducting coil, and others close to the STM. All wiring is made of twisted pairs inserted into stainless steel capillaries, with a large capacitance to ground (around 1 nF/m). Wires are thermalized at the 1 K pot, the still, the mixing chamber, and again on the copper support prior to reaching the STM. We use the same scanning head as in previous work[36] (Fig. 3). The piezotube is located on a moving prism (B in Figs. 1 and 3), which is attached with a strong spring to the base (C in Fig. 3). We use shear piezostacks at two sides of the prism (each consisting of five Ferroperm shear plates glued with Stycast of 10 mm length, 5 mm width, and 0.5 mm thickness each), leaving the side opposite to the spring free for connections. The stacks are driven by a ± 140 V conventional sawtooth signal to provide for conventional coarse approach. The piezotube (we use a Ferroperm piezotube with 0.01 in. wall thickness and 0.5 in. length) allows for scanning ranges up to 2 μm below 4.2 K. The tip (A in Fig. 3) is glued using a small amount of silver epoxy on an M1 screw with a hexagonal head, which is screwed on an M1 bolt glued using Stycast 2850 FT at the piezotube. The positioning device described in the following (D–I in Fig. 3) is screwed below in such a way as to locate the tip on top of the sample holder (E in Fig. 3).

III. DESCRIPTION OF THE POSITIONING DEVICE AND RESULTS

The positioning device (Fig. 3) consists of a sample holder screwed on a slider (E) fixed to a frame (D) at the bottom and from one side with strong springs (F and G). The frame is itself firmly screwed into the main microscope frame (D). The whole system is attached (using Kevlar ropes) to a copper support in good contact with the mixing chamber of the dilution refrigerator [Fig. 3(c)] in such a way as to impede motion of the microscope when pulling on the slider. Frame and slider are made of Ti. Alumina covered with graphite are glued on the bottom of the slider and on the top of the lane

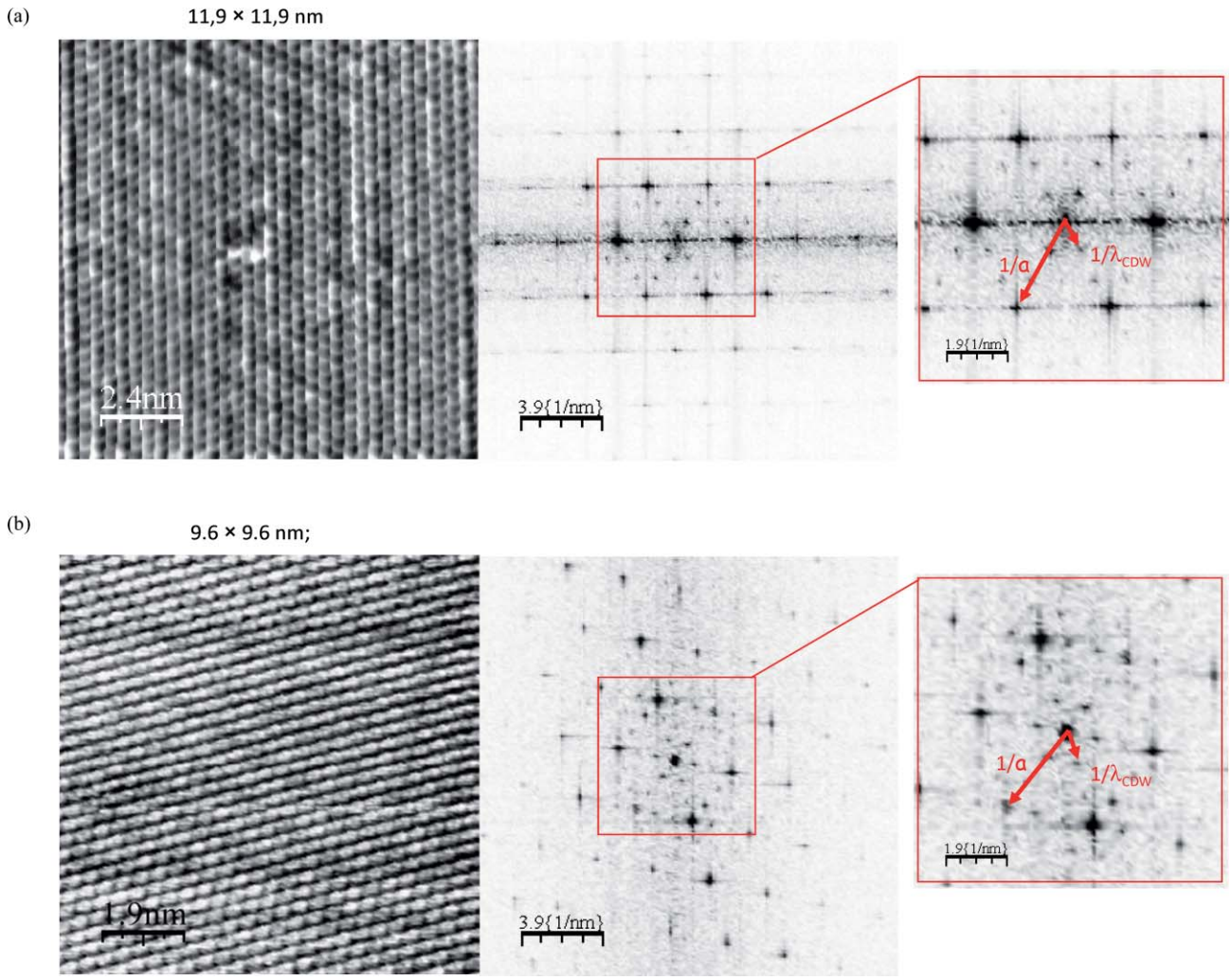

FIG. 4. (Color online) Atomic scale topography taken at zero field (a) and under a magnetic field of 8 T (b) in the compound $NbSe_2$. These images have been taken at 100 mK with the device described here. The grey scale in (a) corresponds to a corrugation of 0.15 nm. Tunneling current was of 10 nA and the voltage bias 50 mV. In the right panels, we show a Fourier transform of the topography, which shows the characteristic sixfold pattern of atomic corrugation at wavevectors corresponding to the inverse of interatomic spacing (a). Around each Bragg peak, small sixfold peaks appear due to the charge density wave modulation at $1/\lambda_{CDW}$. Arrows point to the lattice Bragg peaks ($1/a$) and the CDW modulation ($1/\lambda_{CDW}$).

where the slider moves. The slider is pulled with a multistrand Kevlar rope of 0.1 mm in diameter (I), itself attached, before reaching the mixing chamber, to a stainless steel wire with 0.1 mm diameter (K). The stainless steel wire is maintained stressed using another spring (J) which is attached to the copper support on which the whole microscope assembly is located (M). The wire is soldered to several copper wires in good contact with various fixed temperature locations of the refrigerator (L), namely, in the mixing chamber, the heat exchangers, the still, and at the 1 K pot. It then goes up to room temperature, where a simple linear motion mechanism allows for pulling on the wire.

The mechanical stability of the setup is not influenced by the presence of the positioning device. In Fig. 4, we show atomic scale topography taken at zero field and at a magnetic field of 8 T on two different locations on the layered material $NbSe_2$. Spectroscopy and temperature dependent studies are not influenced by the positioning device and give same results as in previous work.[36] The atomic resolution features are clearly resolved, showing features previously discussed,[39,40] such as the characteristic charge density wave (CDW) order present in $NbSe_2$, as in a large number of previous STM measurements. Note that the CDW wavevector does not change with the magnetic field, being $1/\lambda_{CDW} = 1/3a \pm 1\%$, where a is the lattice constant.

The device has been tested using nanofabricated metallic structures. In Fig. 5(a) we show a scanning electron microscope image over 400 nm wide tracks patterned using focused ion beam on a thin film (200 nm thickness) of Au.[37] The tip was positioned carefully at room temperature using an optical microscope at the edge of a nanopatterned area of about 20 μm × 20 μm. During cool down, the tip stood at approximately the same position, demonstrating that the drift is at most of some μm. The STM images of the nanostructures are shown in Fig. 5(b). The evaporated Au presents the characteristic irregular surface of Au depositions, and the tracks appear as a small depletion, covered in some positions by small Au particles. Three consecutive STM images, taken after subsequently moving the positioning device are shown in the figure. The images have been arranged together to see

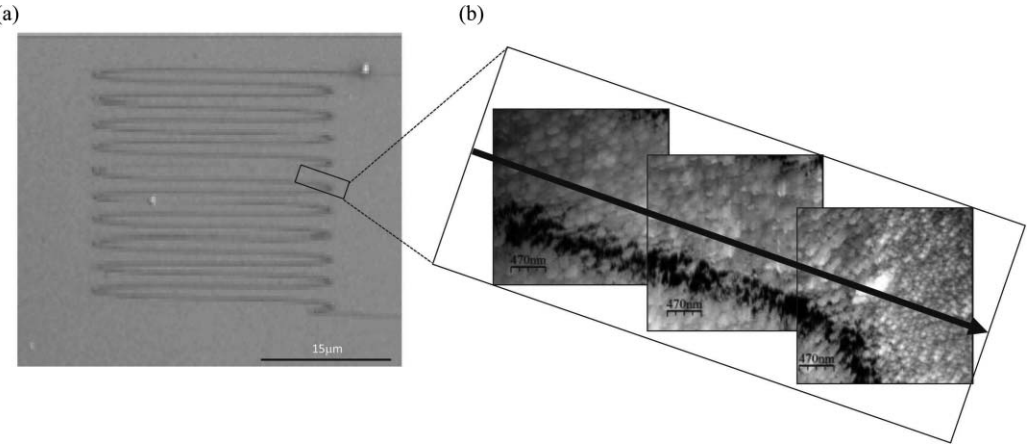

FIG. 5. In (a), we show a SEM image of a pattern nanofabricated with a focused ion beam on top of an Au film. In (b) we show several consecutive images taken with the STM when moving the sample holder with the sliding assembly at 100 mK. Tunneling current and voltage bias are of 8 nA and 5 mV. Height changes represented in the grey scale correspond to a corrugation of 20 nm. Note that the typically grain like topography in gold changes along the direction of the arrow. This is the result of the exposure of the Au film to the focused ion beam, which disappears when going out of the patterned region (image at the right).

the overall direction of motion, represented by a line. Clearly, the 400 nm wide lines and the curvature appearing due to the scan of the focused ion beam are seen on the STM images. Each step corresponds to a movement of around 2 μm, but much smaller steps in the tens of nm range have been reproducibly made. No measurable increase in temperature has been observed during operation of the slider at the base temperature (100 mK).

The positioning system does not increase the mechanical noise of the STM head. In particular, the noise on the tunneling current remains at the same level, without noticeable change when the macroscopic positioning unit is used. The Fourier transform of the current fluctuations are shown in Fig. 6 at 100 mK, with and without operating the positioning system. The noise level observed in the figure represents

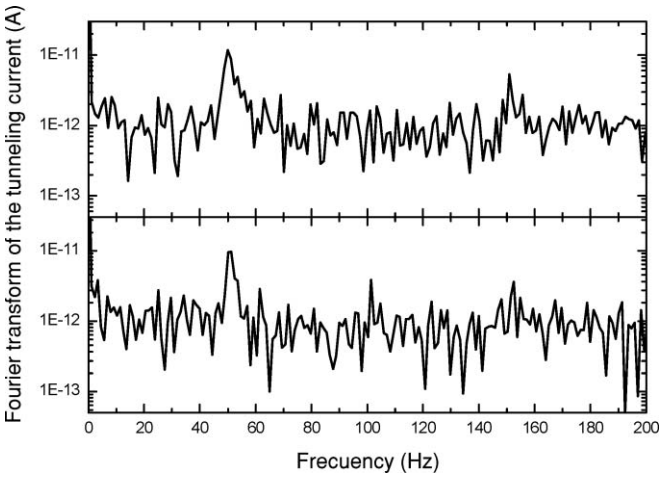

FIG. 6. Fourier transform of a record of the tunneling current as a function of time during 1 s, with the feedback loop switched off at 100 mK and with a magnetic field of 5 T (mean value of tunneling current is of 1.2 nA, and bias voltage is of 100 mV, tip and sample are of Au). Line in upper panel is measured on the STM setup without the positioning setup described here, and line in bottom panel is taken with the macroscopic positioning device and the slider at an intermediate position, with the pulling rope on tension.

a movement of the tip with respect to the sample of around 5 p.m. Therefore, possible vibrations of the wire at room temperature are effectively damped out by the mechanism used for motion. Damping occurs through the combination of the spring which maintains the stainless steel wire in a state of tension (J in Fig. 3), its connection to several metal parts of the cryostat, which should damp out motion through mutual friction between metal surfaces,[38] and the Kevlar rope (I in Fig. 3), which has multiple strands and should also act as a damper. On the other hand, this arrangement significantly improves the mechanical contact between the tip and the sample because much stiffer strings can be used than those typically needed for a stip-slick or inertial motor. This makes the sample holder rather insensitive to low frequency vibrations.

But it has also important additional advantages. It is easy to mount, within the same sample holder, different samples. If one sample is of the same material as the tip, the tip can be *in situ* prepared and shaped following the repeated indentation method previously discussed in Ref. 41. As a matter of fact, we did prepare the tip in a sample of Au in the experiments discussed above and went reproducibly several times back and forth to the sample. The positioning system also allows to apply *in situ* a strong force to a sample, to eventually break it. We have cleaved or broken *in situ* several kinds of samples by locating a knife on the path of the slider.[42] We use a nonmagnetic ceramic blade. For layered materials such as $NbSe_2$, a rod is glued on top of the surface. The rod is then pushed when moving through the blade, freeing a clean surface. After that, or after breaking a single crystallite, the remaining part of the sample is usually thrown away from the STM down to the bottom of the cryostat.

IV. SUMMARY AND CONCLUSIONS

We have presented a dilution refrigerator, high magnetic field, STM setup, which features rapid sample change turn around times, and a simple construction and wiring. The STM has a new coarse motion device for operation at very low temperatures. We have shown that this device can be used

to change the position over the sample with an accuracy of tens of nm and at a range only limited by the available space within the refrigerator as well as to cleave hard single crystal samples at low temperatures. The device can be used to reproducibly position a sample without heat dissipation at temperatures down to 0.1 K. Accuracy and mechanical stability of positioning device have been proven showing position changes over small lines patterned with focused ion beam on a Au film, and atomic scale operation at 8 T and 100 mK in $NbSe_2$. The mechanical rigidity of the local probe–sample system can be significantly increased, with respect to displacers using piezoelectric motors, which improves considerably mechanical noise levels of the STM.

ACKNOWLEDGMENTS

We acknowledge R. Cordoba, J. Sese, J. M. De Teresa, and M. R. Ibarra for preparing focused ion beam nanostructured samples. The STM and cryogenics was partially built and designed at the workshop of UAM, and we acknowledge the help of M. Pazos and A. Buendía. The Laboratorio de Bajas Temperaturas is associated to the ICMM of the CSIC. This work was supported by the Spanish MICINN (Consolider Ingenio Molecular Nanoscience CSD2007-00010 program, MAT2008-06567-C02, FIS2008-00454, and ACI-2009-0905), by the Comunidad de Madrid through program Nanobiomagnet, and by NES program of the ESF.

[1] H. F. Hess, R. B. Robinson, R. C. Dynes, J. M. Valles, and J. V. Waszczak, Phys. Rev. Lett. **62**, 214 (1989).
[2] M. D. Upward, J. W. Janssen, L. Gurevich, A. F. Morpurgo, and L. P. Kouwenhoven, Appl. Phys. A: Mater. Sci. Process. **572**, S253 (2001).
[3] N. Moussy, H. Courtois, and B. Pannetier, Rev. Sci. Instrum. **72**, 128 (2001).
[4] T. Hanaguri, C. Lupien, Y. Kohsaka, D. H. Lee, M. Azuma, M. Takano, H. Takago, and J. C. Davis, Nature **430**, 1001 (2004).
[5] T. Matsui, H. Kambara, and H. Fukuyama, J. Low Temp. Phys. **121**, 803 (2000).
[6] A. E. Gildemeister, T. Ihn, C. Barengo, P. Studerus, and K. Ensslin, Rev. Sci. Instrum. **78**, 013704 (2007).
[7] I. B. Altfeder and A. P. Volodin, Rev. Sci. Instrum. **64**, 3157 (1993).
[8] Y. J. Song, A. F. Otte, Y. Kuk, Y. Hu, D. B. Torrance, P. N. First, W. A. de Heer, H. Min, S. Adam, M. D. Stiles, A. H. MacDonald, and J. A. Stroscio, Nature **467**, 185 (2010).
[9] Y. J. Song, A. F. Otte, V. Shvarts, Z. Zhao, Y. Kuk, S. R. Blankenship, A. Band, F. M. Hess, and J. A. Stroscio, Rev. Sci. Instrum. **81**, 121101 (2010).
[10] T. Prouve, H. Godfrin, C. Gianese, S. Triqueneaux, and A. Ravex, J. Low Temp. Phys. **148**, 909 (2007).
[11] Cryobitz, http://www.cryobitz.de.
[12] G. Binnig and D. Smith, Rev. Sci. Instrum. **57**, 1688 (1986).
[13] R. Smit, R. Grande, B. Lasanta, J. Riquelem, G. Rubio-Bollinger, and N. Agrait, Rev. Sci. Instrum. **78**, 113705 (2007).
[14] T. Berghaus and P. Klaede, U.S. patent 5,237,238 (1993).
[15] S. Pan, E. Hudson, and J. Davis, Rev. Sci. Instrum. **70**, 1459 (1999).
[16] S. H. Pan, International Patent Publication Number WO 93/19494 (International Bureau, World Intellectual Property Organization), 30 September 1993.
[17] J. Lyding, S. Skala, J. Hubacek, R. Brockenbrough, and G. Gammie, Rev. Sci. Instrum. **59**, 1897 (1988).
[18] C. Wittneven, R. Dombrowski, S. Pan, and R. Wiesendanger, Rev. Sci. Instrum. **68**, 3806 (1997).
[19] G. Mariotto, M. D'Angelo, and I. Shvets, Rev. Sci. Instrum. **70**, 3651 (1999).
[20] M. Kugler, C. Renner, V. Mikheev, G. Batey, and O. Fisher, Rev. Sci. Instrum. **71**, 1475 (2000).
[21] A. Schmid and O. Schaff, U.S. patent 6,849,989 (2002).
[22] C. Dubois, P. Bisson, A. Manuel, O. Fisher, and S. Reymond, Rev. Sci. Instrum. **77**, 043712 (2006).
[23] D. Haft, T. Lindenberg, and C. Boedefeld, United States Patent Application 20080148589 (2008).
[24] W. Wang and W. Lu, Rev. Sci. Instrum. **80**, 085104 (2009).
[25] S. Vieira, M. Ramos, and R. Villar, Jpn. J. Appl. Phys. **26-3**, 1711 (1987).
[26] S. Vieira, M. Ramos, M. Hortal, and A. Buendia, Surf. Sci. **181**, 376 (1987).
[27] Y. Kuk and P. Silerman, Rev. Sci. Instrum. **60**, 165 (1989).
[28] S. Chang and S. Li, Rev. Sci. Instrum. **70**, 2776 (1999).
[29] See e.g., http://www.physikinstrumente.com/.
[30] See e.g., http://www.oxford-instruments.com.
[31] J. Jacobs, Adv. Cryog. Eng. **8**, 1963 (1963).
[32] See http://www.airliquide.com.
[33] See, e.g., http://www.lakeshore.com/.
[34] See, e.g., http://www.temati-uk.com/html/performance.html.
[35] H. Suderow, J. Brison, C. Marcenat, and B. Salce, J. Phys.: Condens. Matter **8**, 999 (1996).
[36] H. Suderow, S. Vieira, J. D. Strand, S. Bud'ko, and P. C. Canfield, Phys. Rev. B **69**, 060504(R) (2004).
[37] I. Guillamón, H. Suderow, S. Vieira, A. Fernández-Pacheco, J. Sesé, R. Córdoba, J. M. De Teresa, and M. R. Ibarra, New J. Phys. **10**, 093005 (2008); J. M. De Teresa, A. Fernández-Pacheco, R. Córdoba, J. Sesé, M. R. Ibarra, I. Guillamón, H. Suderow, and S. Vieira, Mater. Res. Soc. Symp. Proc., 1180-CC04-09 (2009).
[38] See, e.g., http://www.scribd.com/doc/2742128/Understanding-the-complex-nature-of-piano-tone.
[39] W. Sacks, D. Roditchev, and J. Klein, Phys. Rev. B **57**, 13118 (1998).
[40] Z. Dai, Q. Xue, Y. Gong, C. G. Slough, and R. V. Coleman, Phys. Rev. B **48**, 14543 (1993).
[41] J. G. Rodrigo, H. Suderow, S. Vieira, E. Bascones, and F. Guinea, J. Phys.: Condens. Matter **16**, R1151 (2004).
[42] H. Sakata, M. Oosawa, K. Matsuba, N. Nishida, H. Takeya, and K. Hirata, Phys. Rev. Lett. **84**, 1583 (2000).